ISSN 1063-7834, Physics of the Solid State, 2007, Vol. 49, No. 5, pp. 868–873. © Pleiades Publishing, Ltd., 2007.
Original Russian Text © A.A. Mazilkin, B.B. Straumal, S.G. Protasova, O.A. Kogtenkova, R.Z. Valievv, 2007, published in Fizika Tverdogo Tela, 2007, Vol. 49, No. 5, pp. 824–829.

DEFECTS AND IMPURITY CENTERS, DISLOCATIONS, AND PHYSICS OF STRENGTH

Structural Changes in Aluminum Alloys upon Severe Plastic Deformation

A. A. Mazilkin, B. B. Straumal, S. G. Protasova, O. A. Kogtenkova, and R. Z. Valiev

Institute of Solid-State Physics, Russian Academy of Sciences, Chernogolovka, Moscow oblast, 142432 Russia
e-mail: mazilkin@issp.ac.ru

Received September 11, 2006

Abstract—The structure and phase composition of Al–Zn, Al–Mg, and Al–Mg–Zn alloys were studied before and after severe plastic deformation of these alloys. The deformation was performed by torsion under high pressure with true strain of ~6. It was established that, as a result of severe plastic deformation, the grains of Al and Zn and also of the β and τ phases revealed in the structure decrease significantly in size and reach nanometer scales. A supersaturated solid solution of Zn in Al decomposes completely in this case and achieves the equilibrium state corresponding to room temperature. The decomposition is less pronounced for the magnesium-containing alloys. Based on the obtained experimental data, a conclusion is drawn concerning the possible mechanisms of this process. Microhardness measurements revealed softening of the alloys as a result of the deformation, which is due to the decomposition of the supersaturated solid solution.

PACS numbers: 61.82.Bg, 66.30.Jt, 62.20.Fe

DOI: 10.1134/S1063783407050113

1. INTRODUCTION

Currently, the fabrication of materials with ultrafine-grained (UFG) structure is one of the new and promising methods of improving material properties. These materials exhibit, for example, a higher strength as compared with conventional coarse-grained materials and, simultaneously, retain a high level of ductility. Among the methods of producing UFG materials, methods of severe plastic deformation (SPD), such as equal-channel angular pressing and torsion under high pressure, are of particular interest. In comparison with commonly used technologies of deformation treatment of materials (rolling, extrusion), the SPD methods permit one to produce bulk nanostructural materials that cannot be produced by conventional thermomechanical treatment. For example, we can cite the production of supersaturated Al–Fe alloys [1] and disordering or even amorphization of intermetallic compounds [2]. However, the role played by the processes that accompany SPD (particularly, diffusion) is unclear. As a result of large plastic deformations, numerous defects form in a material. Therefore, we may assume that, at certain temperatures, recovery processes may occur simultaneously with the deformation.

The aim of this work is to study the role played by diffusion-controlled processes in the formation of the structure and properties of Al-based alloys such as Al–Mg, Al–Zn, and Al–Mg–Zn upon SPD. These systems were chosen primarily due to the fact that they are the basis of many commercial alloys, including superplastic alloys. It is also important that, in the literature, there is a great body of data on the diffusion characteristics of these systems and, in particular, their dependence on pressure [3, 4].

2. EXPERIMENTAL TECHNIQUE

Using vacuum induction melting, we prepared seven aluminum alloys: five binary alloys (10, 20, or 30% Zn; 5 or 10% Mg) and two ternary allows (2% Mg and 5% Zn; 4% Mg and 10% Zn); here and below, alloy compositions are given in wt %. High-purity components were used (5*N*5 Al, 5*N* Zn, 4*N*5 Mg). Alloy samples in the form of discs 0.3 mm thick and 10 mm in diameter were deformed by torsion under high pressure at room temperature [5]. The sample was placed between two dies; the bottom die was rotated, and the upper die was fixed. The pressure applied was 5 GPa. The strain was determined by the number of die revolutions N ($N = 0.5, 1, 2, 5$). The true logarithmic degree of deformation was $\gamma = \ln(2\pi RN/l) \approx 6$ (here, R and l are the radius and the thickness of the sample, respectively, and $N = 5$), and the deformation time was 300 s. The sample temperature during deformation was not above 50°C due to the large mass and high heat conductivity of the dies [5].

The alloy samples were studied by transmission electron microscopy with a JEM-4000FX microscope before and after deformation. We also performed x-ray diffraction studies using a SIEMENS–500 diffractometer (CuK_α radiation). The lattice parameters of the alloys were determined using the x-ray reflections located in the precision angular range of reflection angles $2\theta > 100°$ and the Nelson–Riley extrapolation procedure [6]. The relative error of determining the lattice parameter was less than 0.01%. The samples for study were cut at a distance of 5 mm from the center of a deformed disc. The alloy microhardness was mea-

Table 1. Dependence of the lattice parameter a (in nanometers) of the (Al) solid solution on the concentration of alloying elements in Al–Zn, Al–Mg, and Al–Zn–Mg alloys measured before and after deformation

Composition		Al–Zn			Al–Mg		Al–Mg–Zn	
		10% Zn	20% Zn	30% Zn	5% Mg	10% Mg	2% Mg–5 Zn	4% Mg–10% Zn
Initial state		0.40468	0.40448	0.40444	0.40780	0.40911	0.40578	0.40625
Deformed state	$N = 0.5$			0.40944				
	$N = 1$			0.40496				
	$N = 2$			0.40495				
	$N = 5$	0.40495	0.40496	0.40495	0.40716	0.40890	0.40556	0.40606

sured on a Nanoindenter (MTS Nano Instruments) apparatus with a trihedral pyramid having the same "indentation area/depth" ratio as that of the Vickers indenter. The apparatus has a load resolution of 50 nm and a spatial resolution of 0.01 nm. For each point, we performed no less than 15 measurements. The relative error of determining the microhardness did not exceed 10%. The indentation size was 10–12 μm. It should be noted that the measurements were performed in the same portion of the sample for which the structural data were obtained.

3. RESULTS AND DISCUSSION

3.1. Structural Studies

Based on x-ray diffraction data, we showed in [7] that the structures of all three types of alloys contain an aluminum-based solid solution (which is referred to as (Al) in what follows). The Al–Zn alloys are two-phase; specifically, they contain the Zn phase. In the Al–Mg and Al–Mg–Zn alloys, no other phases were detected, which may indicate that their volume fractions are small. For the alloys under study, the dependence of the lattice parameter of the (Al) solid solution on the alloying-element content in the alloy was determined both before and after deformation (the number of die revolutions upon deformation was $N = 5$). Table 1 lists the measured results for the alloys studied. In the initial state of the Al–Zn system (before deformation), the solid-solution lattice parameter decreases continuously as the Zn content in the alloy increases. The deformation results in an increased (Al) lattice parameter as compared with that in the initial state. The resulting lattice parameter is practically independent of the Zn content in the alloy and is close to that of pure aluminum. Analogous measurements performed for the Mg-containing alloys show that, as the deformation increases, the (Al) lattice parameter decreases, likewise approaching that of pure aluminum. However, this variation is not as significant as in the case of the Al–Zn alloys.

Based on our results on the (Al) lattice parameter and the data from [8], we estimated the contents of Zn and Mg in the (Al) solid solution. In the undeformed alloys with 10, 20, and 30% Zn, the solid solutions contain 6, 12, and 15% Zn, respectively. In the undeformed alloys with 5 or 10% Mg, the Mg content in the solid solution is close to 4 and 8%, respectively. As a result of deformation, the Zn content in the (Al) solution in the Al–Zn alloys decreases sharply and does not exceed 1%. In the two other types of alloys, the content of the alloying elements in (Al) also decreases; however, as noted above, the decrease is not so significant. According to the data on the phase equilibrium in the Al–Zn and Al–Mg alloys, the solubility of Zn and Mg in Al does not exceed 1% at room temperature [9]. In other words, the (Al) solid solution in the initial alloys is in a supersaturated state. Due to deformation, the system passes to a state that is closer to thermodynamic equilibrium than the initial state was. The data for the Al–30% Zn alloys with different degree of deformation (Table 1) suggest that this system reaches an equilibrium state very quickly; namely, practically complete decomposition of the supersaturated solid solution occurs even at $N = 0.5$.

Electron microscopy studies show that the grains in the alloys become significantly smaller due to deformation. Figure 1 shows the structure of the Al–10% Zn alloy after $N = 5$ deformation. In this structure, there are grains of two phases: (Al) grains ~600 nm in size (before deformation, 500 μm) and (Zn) grains ~200 nm in size (before deformation, 3–5 μm). The (Al) grains are equiaxial and have well-defined extinction contours and a dislocation density of $\sim 10^{12}$ m^{-2}, which is low for such a large deformation. This structure is more typical of hot working, whereas the treatment temperature of the sample studied was not above 50°C.

In the Al–Mg and Al–Zn–Mg alloys, the deformation leads to the formation of a similar structure (Figs. 2a and 2b, respectively). The average grain size in the Al–Mg alloys is 150 and 90 nm for the alloys with 5 and 10% Mg, respectively. The grain size in the Al–5% Zn–2% Mg alloy and the Al–10% Zn–4% Mg alloy is 150 and 120 nm, respectively (before deformation, 500 μm). The alloy structures are characterized by a high dislocation density ($>10^{14}$ m^{-2}). According to the electron diffraction data, the alloy structures in both the initial and deformed states contain intermetallide phases, namely, the β phase (Al_3Mg_2) in the Al–Mg system and the τ phase ($Mg_{32}(ZnAl)_{49}$) in the Al–Zn–Mg system. In

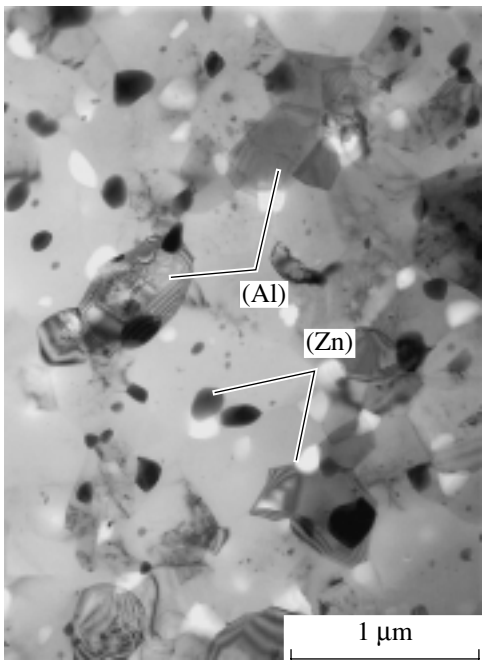

Fig. 1. Microstructure of the Al–10% Zn alloy after severe plastic deformation. Arrows show (Al) and (Zn) grains.

the deformed samples, phase particles about 10 nm in size are uniformly distributed over the material volume.

Thus, for alloys subjected to deformation, we revealed the following: (i) the grain structure is refined and (ii) the (Al) supersaturated solid solution decomposes. The (Al) enriched with Zn is completely decomposed with the formation of the phases corresponding to equilibrium at room temperature. We did not reveal in our samples the Guinier–Preston zones (GPI, GPII) or the α_R' and α_m' phases appearing sequentially during slow decomposition of supersaturated solid solutions [10]. The decomposition of the Mg-containing (Al) solid solution was also observed, but it was less pronounced. In other words, SPD leads to the formation of a phase state that is closer to thermodynamic equilibrium than the initial undeformed state is.

Evidently, the observed decomposition is determined by diffusion mechanisms, namely, volume diffusion and grain-boundary diffusion. Based on the structural data obtained, let us estimate the contributions of these mechanisms to the decomposition of the supersaturated solid solution. Setting the diffusion path equal to 500 nm (the average grain size) and using the deformation duration (300 s), we find the volume-diffusion coefficient to be $D(300\ \mathrm{K}) \approx 4 \times 10^{-15}\ \mathrm{m^2\ s^{-1}}$. The published data on the volume diffusion of Zn in Al give $D(300\ \mathrm{K}) \approx 1.0 \times 10^{-22}\ \mathrm{m^2\ s^{-1}}$ [11, 12]. For the Mg diffusion in Al single crystals, we have $D(300\ \mathrm{K}) \approx 1.7 \times 10^{-24}\ \mathrm{m^2\ s^{-1}}$. It is seen that both of these values are 8 to 9 orders of magnitude lower than our estimate. Thus, the volume diffusion cannot account for the decomposition of the supersaturated solid solution due to deformation.

The decomposition of the (Al) solid solution may also be controlled by grain-boundary diffusion of Zn and Mg atoms. Indeed, impurities in the solution are arranged along dislocations formed during deformation, and the redistribution of dislocations leads to the formation of new grain boundaries. Therefore, these boundaries will be significantly enriched with Zn and Mg. The grain-boundary diffusion is characterized by the so-called triple product $sD_b\delta$ (s is the segregation coefficient, D_b is the grain-boundary diffusion coefficient, and δ is the boundary width). The experimental determination of D_b is a fairly difficult problem, and only several direct measurements of this quantity have been performed. However, calculations show that the ratio $D_b/D \sim 10^2$ [14]. Based on this estimate and setting $\delta = 0.5$ nm and $s = 1$, we find the grain-boundary diffusion coefficient to be $sD_b\delta = 2 \times 10^{-22}\ \mathrm{m^3\ s^{-1}}$. Extrapolation of the available data to $T = 300$ K gives $sD_b\delta = 3 \times 10^{-24}\ \mathrm{m^3\ s^{-1}}$ for Zn and $5 \times 10^{-28}\ \mathrm{m^3\ s^{-1}}$ for Mg. It is seen that the difference between the literature data and our estimates for Zn is significantly less than in the case of volume diffusion. Nevertheless, the grain-boundary diffusion likewise cannot account for the decomposition of the supersaturated solid solution.

We should also include the effect on diffusion of other two factors in materials subjected to plastic deformation, namely, nonequilibrium vacancies and elevated pressure. These factors act in opposite directions: excess vacancies accelerate diffusion, while pressure slows it down. Electron-microscopic observations of the formation of vacancies performed in situ during deformation of copper [15] and gold [16] showed that the excess vacancy concentration can reach values 10^{-5}–10^{-4} at a strain of $e \approx 1$, which is comparable to the vacancy concentration at the melting point. Thus, in our case ($e \approx 6$), we may expect that the degree of material supersaturation with vacancies can be fairly significant. A second factor is associated with the dependence of the diffusion coefficient on the hydrostatic pressure applied. Under the deformation conditions used, the pressure acting on the sample is not hydrostatic. For an external pressure of 5 GPa, the corresponding component of the spherical stress tensor is ~1.7 GPa. According to [17], this hydrostatic pressure can decrease the diffusion coefficient by at most an order of magnitude.

Based on the above estimates and the experimental data obtained, we may conclude that the most probable mechanism of decomposition of the supersaturated solution in the Al–Zn alloys subjected to deformation is the grain-boundary diffusion accelerated by a nonequilibrium-vacancy flux. An analogous situation occurs in the Al–Mg and Al–Mg–Zn alloys; however, the solution decomposition in them occurs much more slowly under the same conditions. The reason for this may be the lower grain-boundary diffusion coefficient of Mg (which is four orders of magnitude lower than that for Zn).

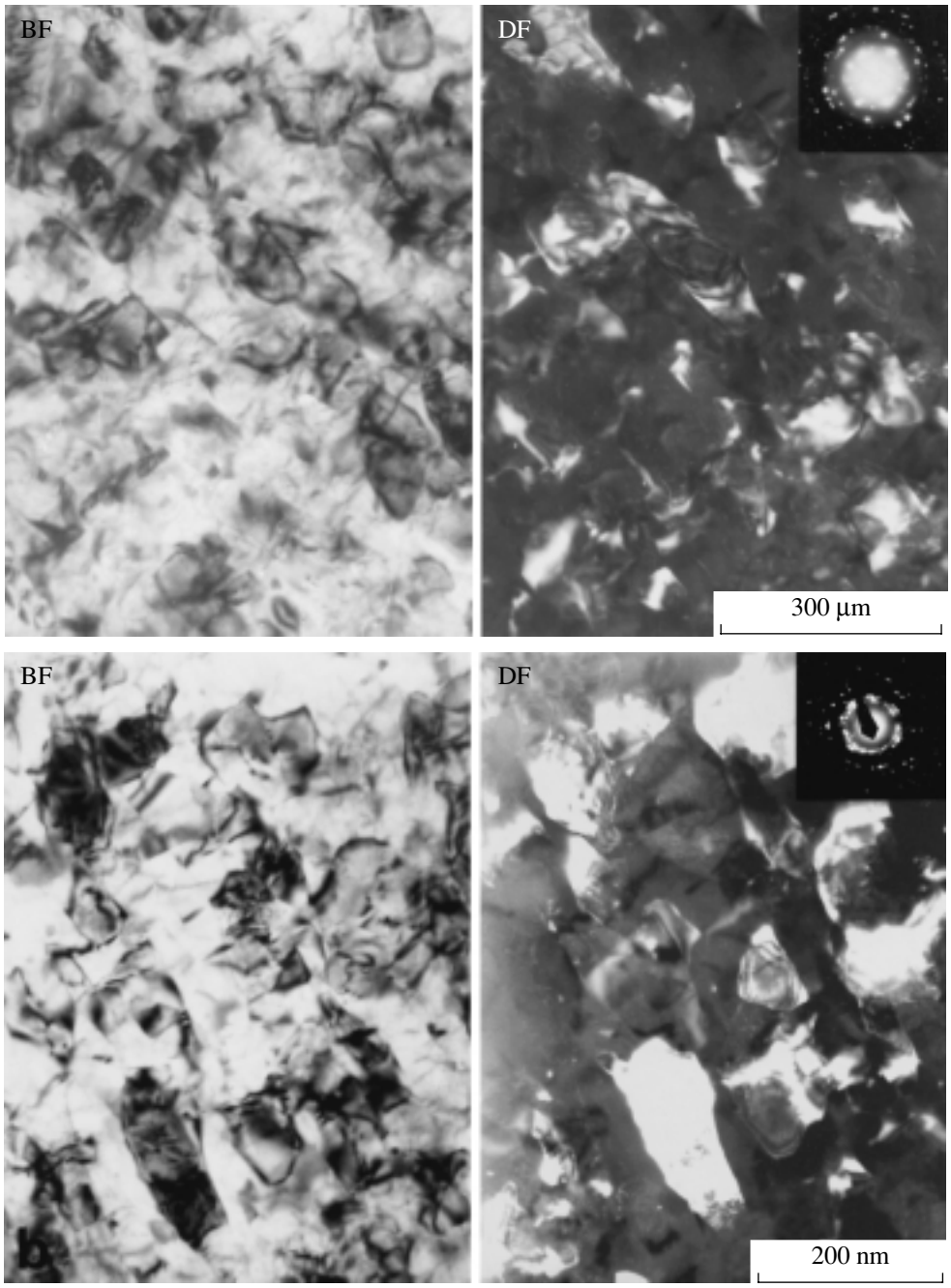

Fig.2. Microstructures of deformed (a) Al–5% Mg and (b) Al–2% Mg–5% Zn alloys. The neighboring photographs show the areas obtained in a bright (BF) and dark (DF) field, respectively.

3.2. Measurement of the Mechanical Properties

To describe the variations in the alloy's mechanical properties as a result of SPD, we measured the alloy microhardness H. The results are presented in Table 2. It is seen that, for all three types of alloys in the initial state, the microhardness increases with the Mg or Zn content. Since the undeformed samples have low dislocation densities (10^{10} m^{-2}) and large grain sizes (about 500 μm, which is much greater than the indentation size), the measured microhardness corresponds to that of the supersaturated solid solution and its increase is due to solid-solution strengthening.

The hardness of the deformed Al–Mg and Al–Mg–Zn alloys increases slightly with the Mg and Zn concentrations, which is likewise explained by the solid-solution strengthening. The deformation of these alloys leads to a small decrease in the microhardness. A more substantial decrease in the microhardness due to deformation is observed in the Al–Zn alloys. Here, it should

Table 2. Dependence of the hardness H (in gigapascals) of Al–Zn, Al–Mg, and Al–Zn–Mg alloys on the concentration of alloying elements measured before and after deformation

Composition		Al–Zn			Al–Mg		Al–Mg–Zn	
		10% Zn	20% Zn	30% Zn	5% Mg	10% Mg	2% Mg–5 Zn	4% Mg–10% Zn
Initial state		0.95	1.55	1.90	2.42	2.78	2.06	1.88
Deformed state	$N = 0.5$			0.59				
	$N = 1$			0.77				
	$N = 2$			0.80				
	$N = 5$	0.84	0.93	0.95	2.32	2.61	2.53	2.25

be noted that the indentation size exceeds the grain size in the deformed alloys. The value of H for them is determined by the solid-solution strengthening, the grain size (the Hall–Petch relationship), and cold hardening.

The fairly unusual behavior of the alloys, namely, the decrease in their strength characteristics instead of strengthening upon deformation, can be explained in terms of the structural variations described above. Indeed, based on the Hall–Petch relationship, one would expect strengthening of the material because the grains become significantly finer. However, the deformation causes not only a decrease in the grain size but also the decomposition of the supersaturated solid solution, with the result that all the excess impurity (as in the Al–Zn alloys) or its part (as in the Al–Mg and Al–Mg–Zn alloys) escapes the solid solution. The variation in the material hardness determined solely by the Hall–Petch relationship was observed in the Al–30% Zn alloys differing in strain (Fig. 3). Indeed, these samples have almost the same degree of solid-solution supersaturation, because, according to the x-ray diffraction data, the solid-solution decomposition is completed at $N = 0.5$ (Table 1). The dislocation densities for all four degrees of deformation are also almost the same. Therefore, the difference in the material hardness is determined solely by the grain size.

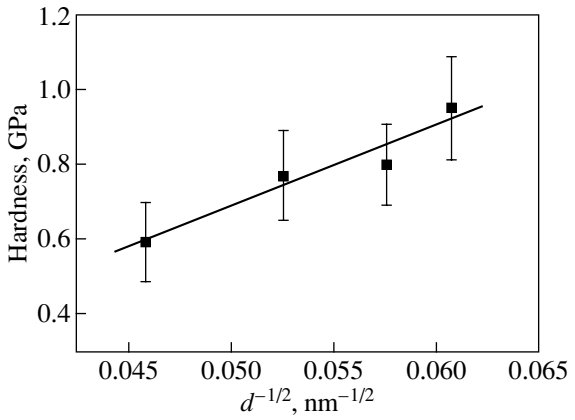

Fig. 3. Hall–Petch dependence for Al–30% Zn alloys differing in strain.

Because the softening due to the decomposition of the supersaturated solid solution dominates over the strengthening due to the decreased grain size and increased dislocation density, the material strength decreases upon deformation. The fact that the solid solution in the Mg-containing alloys decomposes more slowly explains why the softening in these alloys is less pronounced.

4. CONCLUSIONS

(i) Severe plastic deformation of Al alloys significantly decreases the Al and Zn grain sizes and the size of particles of intermetallide phases. As a result of deformation, the supersaturated Al solid solution decomposes and the system passes gradually into the state corresponding to the equilibrium phase diagram.

(ii) The most probable mechanism for the system to achieve the equilibrium state is the grain-boundary diffusion accelerated by the vacancy flux forming upon deformation.

(iii) The hardness of alloys in the initial state increases with the Zn or Mg content owing to the solid-solution strengthening. Upon deformation, the overall effect of cold hardening, softening (due to the decomposition of the supersaturated solid solution), and strengthening (due to the decreased grain size) leads to the decreased hardness of the alloys under study. The most significant softening occurs in the Al–Zn alloys, wherein the supersaturated solid solution decomposes practically completely.

ACKNOWLEDGMENTS

This work was supported by the Russian Foundation for Basic Research (project nos. 06-02-32875 and 05-02-16528) and INTAS (grant nos. 03-51-3779 and 05-109-4951).

REFERENCES

1. V. V. Stolyarov, L. O. Shestakova, Y. T. Zhu, and R. Z. Valiev, Nanostruct. Mater. **12**, 923 (1999).

2. A. V. Korznikov, O. Dimitrov, G. F. Korznikova, J. P. Dallas, A. Quivy, R. Z. Valiev, and A. Mukherjee, Nanostruct. Mater. **11**, 17 (1999).
3. Y. S. Kang, H. Araki, Y. Minamino, T. Yamane, S. Saji, K. Azuma, and Y. J. Miyamoto, Nippon Kinzoku Gakkaishi (J. Jpn. Inst. Met.) **57**, 990 (1993).
4. Y. Fujinaga and T. J. Sato, J. Alloys Compd. **209**, 311 (1994).
5. R. Z. Valiev, R. K. Islamgaliev, and I. V. Alexandrov, Prog. Mater. Sci. **45**, 103 (2000).
6. S. S. Gorelik, L. N. Rastorguev, and Yu. A. Skakov, *X-Ray and Electron-Optical Analysis* (Metallurgiya, Moscow, 1970) [in Russian].
7. A. A. Mazilkin, O. A. Kogtenkova, B. B. Straumal, R. Z. Valiev, and B. Baretzky, Diffus. Defect Data, Pt. A **237–240**, 739 (2005).
8. E. C. Ellwood, J. Inst. Met. **80**, 217 (1952).
9. T. B. Massalski, *Binary Alloy Phase Diagrams* (ASM International, Materials Park, OH, 1993).
10. H. Löffler, *Structure and Structure Development of Alloys* (Akademie, Berlin, 1995).
11. N. L. Peterson and S. J. Rothman, Phys. Rev. B: Solid State **1**, 3264 (1970).
12. I. Gödény, D. L. Beke, and F. J. Kedves, Phys. Status Solidi A **13**, K155 (1972).
13. S. J. Rothman, N. L. Peterson, L. J. Nowicki, and L. C. Robinson, Phys. Status Solidi B **63**, K29 (1974).
14. B. S. Bokshteĭn, S. Z. Bokshteĭn, and A. A. Zhukhovitskiĭ, *The Thermodynamics and Kinetics of Diffusion in Solids* (Metallurgiya, Moscow, 1974) [in Russian].
15. M. Kiritani, K. Yasunaga, Y. Matsukawa, and M. Komatsu, Radiat. Eff. Defects Solids **157**, 3 (2002).
16. M. Kiritani, Mater. Sci. Eng., A **350**, 1 (2003).
17. G. Erdelyi, W. Lojkowski, D. L. Beke, I. Gödény, and F. J. Kedves, Philos. Mag. A **56**, 673 (1987).

Translated by Yu. Ryzhkov

SPELL: OK